Supplementary Information

A novel nickel catalyst supported on fly ash-derived zeolite ZK-14 for CO_2 Methanation via situ reduction

Kaige Chen [a,b], Jie Li [c], Yongxiang Wang [c],Yong Dai [c], Yongming Luo [a,b,*], XiaoHua Cao [a,b,*], Xiaoping Xing [c,*]

a Faculty of Chemical Engineering, Kunming University of Science and Technology, Kunming 650500, PR China

b Key Laboratory of Yunnan Province for Synthesizing Sulfur-containing Fine Chemicals, The Innovation Team for Volatile Organic Compounds Pollutants Control and Resource Utilization of Yunnan Province, The Higher Educational Key Laboratory for Odorous Volatile Organic Compounds Pollutants Control of Yunnan Province, Kunming 650500, PR China

c School of Chemistry and Chemical Engineering Yancheng Institute of Technology, Yancheng 224051, P. R. China

***Corresponding authors.**

environcatalysis@kust.edu.cn (Y. Luo)

xiaohuacao@kust.edu.cn (X. Cao)

xingxiaoping@ycit.cn (X. Xing)

Catalyst characterizations

XRD: X-ray diffraction measurements were performed using a SmartLab diffractometer with a 2θ range of 5º to 90º and a step size of 0.0001º·min^{-1}.

SEM and HRTEM: Scanning electron microscopy images were taken on a Zeiss Supra 40 field-emission scanning electron microscope at 2.0 kV. Transmission electron microscopy images were taken on a Hitachi Model H7700 microscope at 100.0 kV. High-resolution TEM (HRTEM)images, scanning TEM (STEM) images, and energy-dispersive X-ray spectroscopy (EDS) mapping profiles were recorded on an FEI Talos F200X field-emission high-resolution transmission electron microscope at 200.0 kV.

XPS: X-ray photoelectron spectra were collected on an ESCALAB 250 X-ray photoelectron spectrometer, using non-monochromatic Al-Kα X-ray as the excitation source.

EPR: Electron paramagnetic resonance spectra were recorded on a Bruker A300-10/12 spectrometer in Germany, with oxygen defects measured at room temperature.

N_2 adsorption: The surface area was determined based on the nitrogen adsorption isotherm (-196 ºC) using a TriStar II 3020 apparatus. Before measurement, the samples were degassed under vacuum at 200 ºC for 3 hours. The mesopore volume, micropore volume, and surface area were analyzed from the desorption curve using the Barrett-Joyner-Halenda (BJH) model, and the micropore volume was analyzed using the t-plot.

H_2-TPR: H_2-temperature programmed reduction Temperature-programmed reduction curves were recorded using an AutoChem II 2920 apparatus equipped with a high-sensitivity thermal conductivity detector (TCD). The catalyst precursor was first

pretreated in He (30 mL·min^{-1}) at a rate of 10 ^{o}C ·min^{-1} to 100 ^{o}C for 1 hour, then cooled to room temperature. After temperature stabilization, the carrier gas was switched to a H_2/Ar mixture (30 mL·min^{-1}) and purged for 1 hour. Once the baseline stabilized, the temperature was increased at a rate of 10 ^{o}C ·min^{-1} to 900 ^{o}C, with signals recorded ten times per second.

CO_2-TPD: CO_2 temperature-programmed desorption was conducted on the same apparatus (AutoChem II 2920). The material was first reduced in 10% H_2/Ar at 320 ^{o}C and then cooled to 50 ^{o}C. After pretreatment in He (30 mL·min^{-1}) at a rate of 10 ^{o}C ·min^{-1} to 100 ^{o}C for 1 hour and cooling to the adsorption temperature of 50 ^{o}C, the carrier gas was switched to CO_2 at a flow rate of 30 mL·min^{-1} and adsorbed for 1 hour. The carrier gas was then switched to He (30 mL·min^{-1}) and purged for 1 hour. Once the baseline stabilized, the temperature was increased at a rate of 10 ^{o}C ·min^{-1} to 850 ^{o}C, with signals recorded ten times per second. The desorbed CO_2 was measured using a TCD detector.

In situ DRIFTS: In situ DRIFTS was recorded on a Nicolet iS50 FT-IR (Thermo Fisher, America) using an in-situ cell. To further verify the intermediate, the reaction pathway, and the reaction mechanism for CO_2 hydrogenation. The samples were placed in an infrared (IR) reaction chamber, which is specially designed for detecting highly dispersed powder samples in diffuse reflectance mode. After the samples were loaded, the chamber was purged with argon (99.999%) for 30 minutes, and a spectrum was collected as the background spectrum. During in situ characterization, a continuous flow of CO_2 and H_2 mixed gas (20/80 vol%) was introduced into the reaction chamber

at a flow rate of 30 ml·min^{-1}. After heating to 200 ^{o}C, a sample was collected every 20 ^{o}C for 30 minutes.

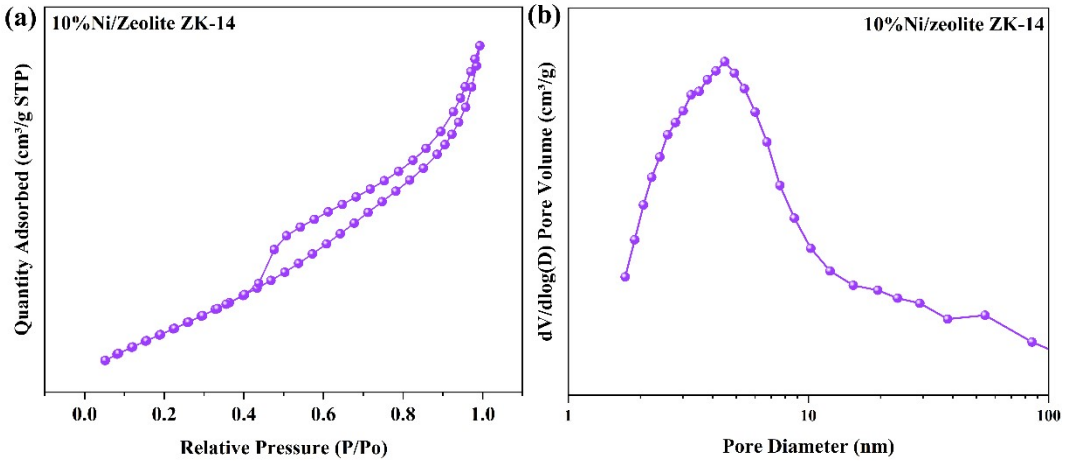

Figure S1 N_2 adsorption/desorption curves (a) and pore size (b) distribution of 10%Ni/zeolite ZK-14.

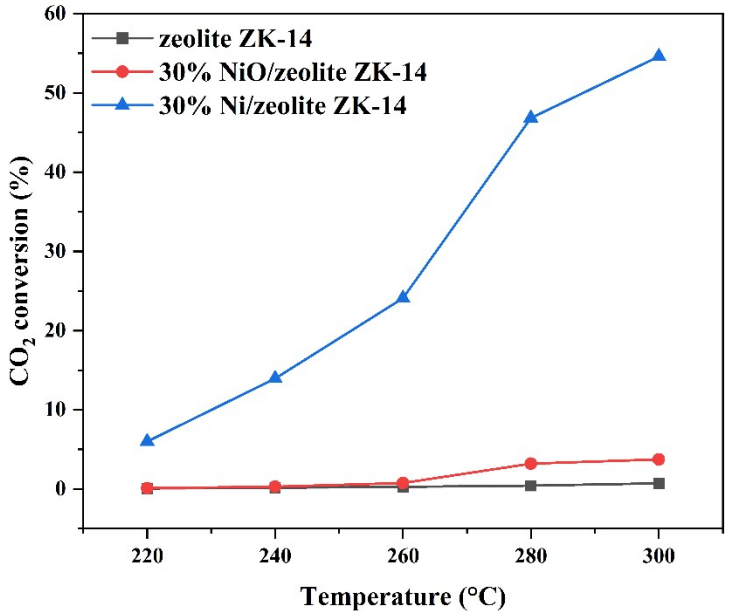

Figure S2 CO_2 conversion versus temperature for zeolite ZK-14, 30%NiO/ zeolite ZK-14 and 30%Ni/ zeolite ZK-14 Catalysts.

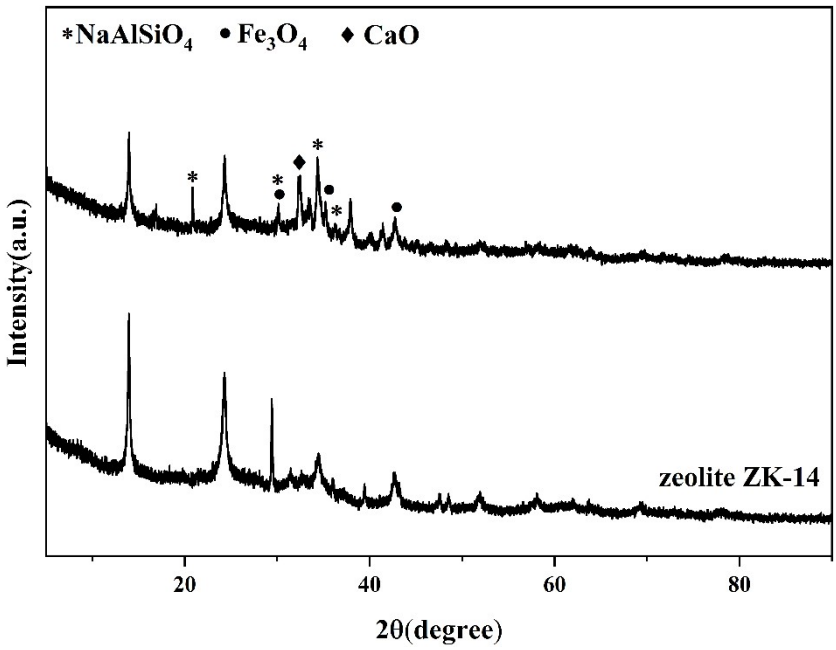

Figure S3 Comparison of zeolite ZK-14 before and after hydrothermal treatment.

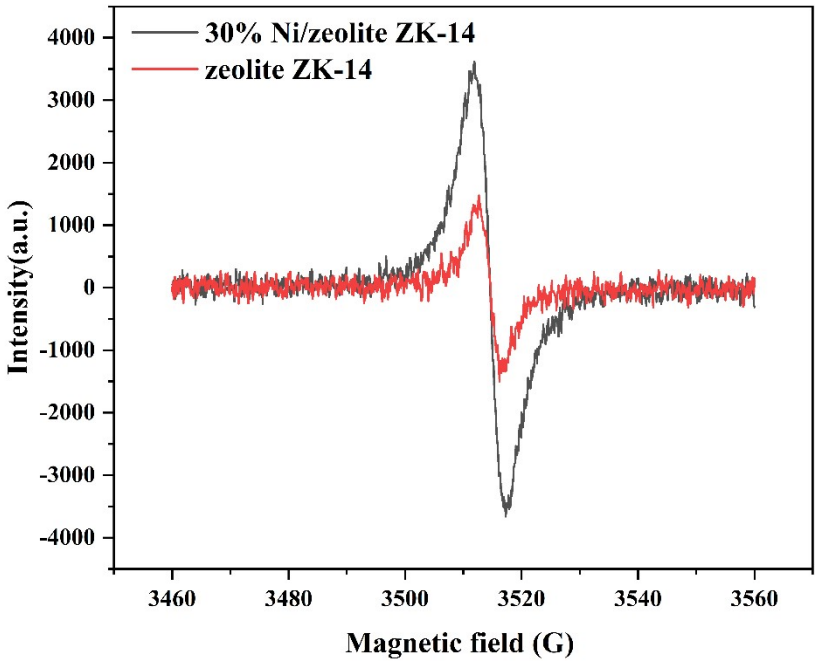

Figure S4 EPR profiles on the zeolite ZK-14 and 30%Ni/zeolite ZK-14.

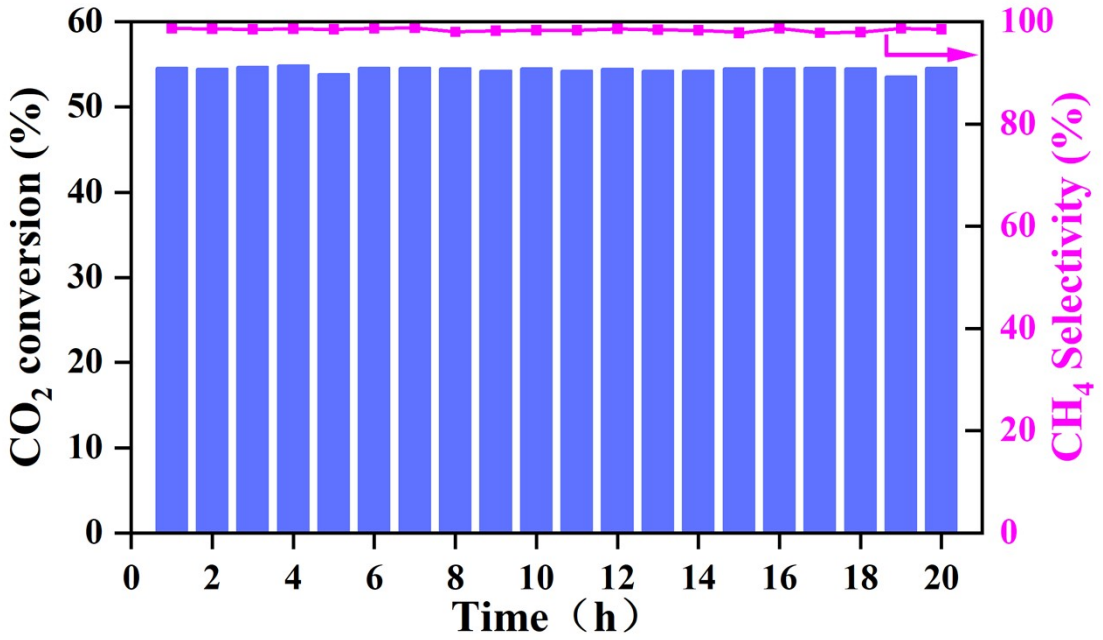

Figure S5 Stability Test of CO_2 Hydrogenation over 30%Ni/zeolite ZK-14 Catalyst at 300 °C.

Table S1 Physical Properties of 30%NiO/ zeolite ZK-14 and 30%Ni/ zeolite ZK-14 Catalysts.

Catalysts	Ni loading[a](wt %)	Ni^0/Ni_{total}[b]	O_B/O_{total}[b]
30%NiO/zeolite ZK-14	25.9	0	16.5%
30%Ni/zeolite ZK-14	25.9	1.64%	40.7%

[a] Measured by ICP-OES. [b] Calculated by the fitted XPS spectra.

Table S2 Main substance content of fly ash analyzed by XRF.

Al_2O_3	SiO_2	K_2O	CaO	TiO_2	Fe_2O_3	SO_3
33.226%	51.517%	2.275%	2.472%	1.256%	5.204%	1.611%

Table S3 ICP-OES of zeolite ZK-14 and 30%Ni/ zeolite ZK-14 Catalysts.

	Ni	Na	Al	Si	Ca	Fe	K
zeolite ZK-14	0	9.691 %	11.977 %	12.629 %	2.697 %	3.250 %	0.528 %
30%Ni/zeolite ZK-14	25.9 %	5.750 %	9.294%	10.409 %	2.140 %	2.434 %	0.326 %

Table S4 Comparison of the different data on Ni supported on zeolite and other nanostructured materials as catalysts for CO_2 hydrogenation.

Catalysts	P(MPa)	Temperature (°C)	GHSV (h^{-1})	CO_2 conversion (%)	CH_4 Selectivity (%)	Source
Ni/Fly ash zeolite X	0.1	300	12000	0	0	1
		450		53	90	
Ni-13X	2	280	13333	50	96	2
Ni-5A		300		35	62	
Ni/NaY	0.1	250	12000	33	100	3
		300		43	100	
Ni/CGLTA-5A	0.1	300	30000	17	80	4
		450		73	91	
Ni/fly ash (CCFA)	0.1	450	20003000	9282	5756	5
Ni/MCM-41	0.1	300	15000	20	95	6
		450		70	70	
Ni/SiO_2	2	310	20000	77.2	100	7
Ni@UiO-66	1	350	1650	48	84	8
Ni@MIL-101	1	320	4650	57	92	8
30%Ni/Zeolite ZK-14	1	280	12000	46.8	98.9	This work
		300		54.6	98.7	

1. N. Czuma, K. Zarebska, M. Motak, M. E. Galvez and P. Da Costa, *Fuel*, 2020, **267**.
2. L. Wei, W. Haije, N. Kumar, J. Peltonen, M. Peurla, H. Grenman and W. de Jong, *Catal. Today*, 2021, **362**, 35-46.
3. N. A. Sholeha, S. Mohamad, H. Bahruji, D. Prasetyoko, N. Widiastuti, N. A. A. Fatah, A. A. Jalil and Y. H. Taufiq-Yap, *RSC Adv.*, 2021, **11**, 16376-16387.
4. S. Bahraminia and M. Anbia, *Int. J. Hydrog. Energy*, 2024, **83**, 842-855.
5. X. Dong, B. Jin, S. Cao, F. Meng, T. Chen, Q. Ding and C. Tong, *Waste Manag.*, 2020, **107**, 244-251.
6. M. C. Bacariza, I. Graca, S. S. Bebiano, J. M. Lopes and C. Henriques, *Chem. Eng. Sci.*, 2018, **175**, 72-83.
7. R.-P. Ye, L. Liao, T. R. Reina, J. Liu, D. Chevella, Y. Jin, M. Fan and J. Liu, *Fuel*, 2021, **285**.
8. M. Mihet, O. Grad, G. Blanita, T. Radu and M. D. Lazar, *Int. J. Hydrog. Energy*,

2019, **44**, 13383-13396.